

MAGNETIC PROPERTIES OF ISABELLE SUPERCONDUCTING QUADRUPOLES*

E. Willen, R. Engelmann, A.F. Greene
J. Herrera, K. Jaeger, H. Kirk, K. Robins
Brookhaven National Laboratory
Upton, New York 11973

A number of superconducting quadrupole magnets have been constructed in the ISABELLE project during the past year.¹ With these quadrupoles, it was intended to test construction techniques, magnet performance and measuring capability in an effort to arrive at a quadrupole design satisfactory for use in the storage ring accelerator. While these magnets are designed to have dimensions and field properties close to those needed for regular cell ISABELLE quadrupoles, no effort was made to make them identical to one another. This report will detail the performance characteristics of one of these magnets, MQ3005.² It must be kept in mind that this report is a "snapshot" of present status and will be soon outdated by continuing developments.

We begin with a brief summary of the measuring techniques and the relevant formalism used in our description of the magnetic field properties of the magnets. The magnetic field within the aperture of the ISABELLE quadrupoles was measured by means of a set of Morgan type coils³ rotating about a common shaft along the axis of magnet. The voltage output from each coil is primarily responsive to one component of the multipole field. Such an arrangement therefore allows one to determine the amplitude of each multipole field and its angular orientation with respect to the median plane of the dominant multipole. Since the total magnetic field is essentially two dimensional we have used a representation in terms of cylindrical harmonics referred to the axis of the quadrupole field, that is, the expansion is made about an axis chosen to minimize the dipole component of the field. Thus, at any point (r,θ) in the aperture, the rectangular components of the total magnetic field are

$$B_y(r,\theta) = \sum_{n=0}^{\infty} \frac{B_{TH}}{G_{TH}} G_o r^n (b_n \cos n\theta - a_n \sin n\theta)$$

$$B_x(r,\theta) = \sum_{n=0}^{\infty} \frac{B_{TH}}{G_{TH}} G_o r^n (a_n \cos n\theta + b_n \sin n\theta)$$

where a_n and b_n are the median plane coefficients,

G_o = the gradient of the quadrupole,

B_{TH} = the design operating dipole field of the lattice dipoles of the ISABELLE rings

G_{TH} = the corresponding operating gradient of the ISABELLE quadrupoles.

When we consider these equations for a field observation point in the median plane of the quadrupole, that is, for $r = x$ and $\theta = 0$, we derive the simplified relations

$$B_y(x) = \frac{B_{TH}}{G_{TH}} G_o (b_o + b_1 x + \dots + b_n x^n)$$

and

$$B_x(x) = \frac{B_{TH}}{G_{TH}} G_o (a_o + a_1 x + \dots + a_n x^n)$$

*Work performed under the auspices of the U.S. Department of Energy.

It will be noted that by placing the factor $(B_{TH}/G_{TH})G_o$ outside the expansions, we have introduced median plane coefficients, a_n and b_n , for the quadrupole magnet which are consistent with those conventionally employed for the ISABELLE dipole magnets. In addition, the resulting multipole coefficients, a 's and b 's, are then, in principle, less sensitive to the operating field level of the quadrupole, since the dominant variations due to iron saturation and hysteresis are carried by the gradient field (G_o) of the quadrupole.

The design injection field for ISABELLE requires a current of ~300 amperes in the magnets.⁴ The current at full field, corresponding to 400 GeV, is 3917 A. The quadrupole magnets are built with a cos 2θ current distribution in the coils, each of which is wound with 47 superconducting turns. The inner coil diameter is 13.09 cm. The quadrupole magnets are designed to have dipole, quadrupole and dodecapole correction coils to control the working parameters of the machine. The design ramp rate for ISABELLE is ~8 A/s.

For quadrupole MQ3005, the design criterion which determines the performance of the magnet is the use of high resistance, superconducting braid⁵ for the coils. High resistance braid is braid which, through various processing techniques, has a larger interstrand resistance than normal braid ($5000 \times 10^{-5} \text{ ohm}$ vs $1 \times 10^{-5} \text{ ohm}$). The objective is to reduce "AC" effects: distortions in field quality due to currents induced as the magnet is ramped up in current.

The quench history for this magnet is shown in Fig. 1. The relatively slow training shown by this magnet is thought to be due to the fact that the coils were built with little epoxy. This was done in order to increase their permeability to cold helium. The low epoxy content had the effect of making the coil mechanically less rigid, and hence the slow training.

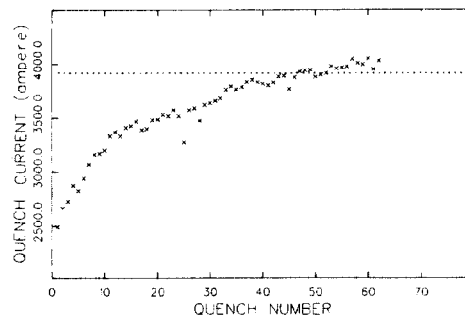


Fig. 1. Quench history of MQ3005. Several of the lower quenches are due to special tests.

Figure 2 shows the transfer function for this magnet as measured under several different conditions. "DC" means that field which is measured after all significant effects induced by ramping have died away (approx. 5 min). The triangles demonstrate that for this magnet, ramping at 8 A/s does not significantly change the transfer function. (This dynamic measurement is possible because the Morgan coil system can make a complete reading of the field in 1/6 s.) The

fall-off in the transfer function at high current is as expected and due to iron saturation. The transfer functions for the data including the magnet ends have been normalized to the DC data excluding the ends at 2000A. Because of the particularly sensitive scale used to display the transfer function, the data is sensitive to noise in the measuring system and in accurate current reads below 500A. We are investigating this lower current region further.

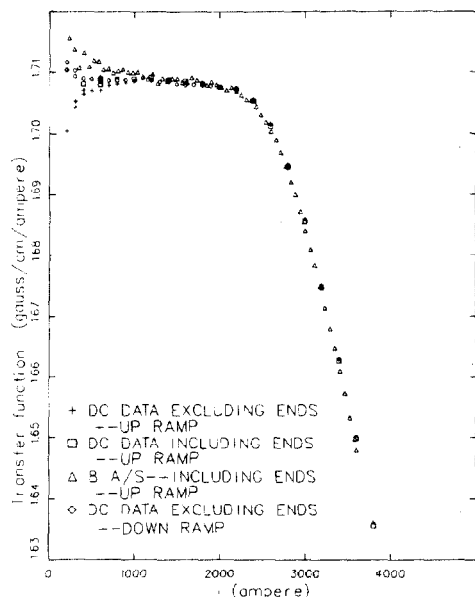


Fig. 2. Quadrupole transfer function for MQ3005.

Figure 3 is a plot of the gradient variation vs current at a fixed position 3 cm from the center of the magnet. Figure 4 shows, for several currents, the field variation across the aperture. Figures 3 & 4 describe the field in the median plane of the magnet. The specified aperture for ISABELLE is 8.8 cm.⁴ The shaded bar on the vertical axis is the permitted magnet-to-magnet RMS variation at 3 cm. The basic quadrupole design looks promising in this respect. To obtain these plots, the permitted RMS variation for the harmonic b_5 , for which correction trim coils are planned, has been used in place of the measured value for b_5 . These plots are made from DC data taken in the center of the magnet.

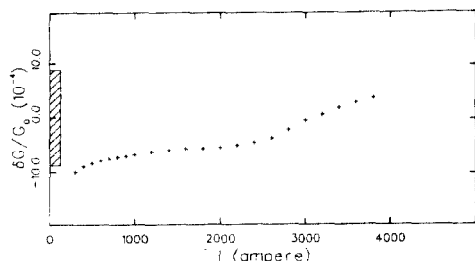


Fig. 3. Gradient variation at $x = 3$ cm on the median plane.

In the following plots, a shaded bar appearing on the vertical axis is the permitted RMS variation for that term. The symbols are defined in Fig. 2. The data are displayed for a magnetic axis along which the dipole term is minimized.

The first allowed harmonic b_5 and the skew component a_5 are shown in Figs. 5a & 5b. The a_5

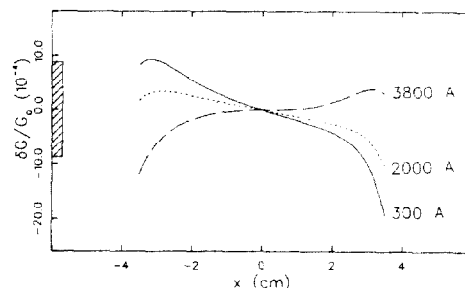


Fig. 4. Gradient variation on the median plane.

coefficient is close to the expected mean value (over many magnets) of zero. The b_5 coefficient displays a sizable contribution from the magnet ends. It is also evident, from the difference between the up-ramp and down-ramp data sets, that there are sizable superconducting magnetization and iron hysteresis effects in this magnet.

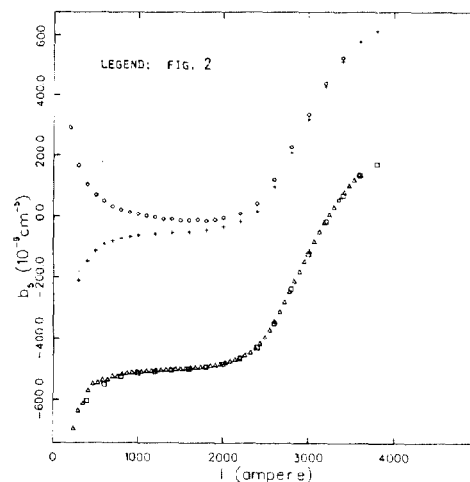


Fig. 5a. Normal dodecapole coefficient.

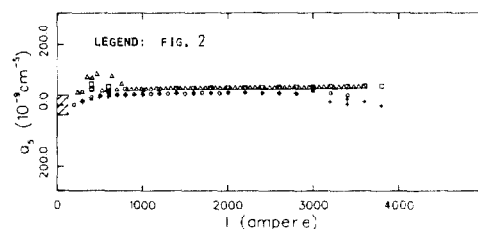


Fig. 5b. Skew dodecapole coefficient.

The next allowed harmonic b_9 and the skew component a_9 are shown in Figs. 6a & 6b. The real significance of these values for b_9 and a_9 will become evident only after more magnets are constructed.

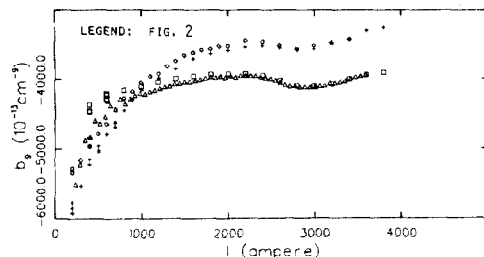


Fig. 6a. Normal 20-pole coefficient.

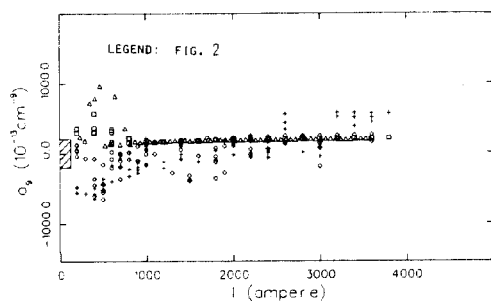


Fig. 6b. Skew 20-pole coefficient.

Of special significance is the observation that the harmonics measured at 8 A/sec are essentially the same as the DC harmonics. This is attributed to the high resistance braid use in the construction of the coils.

The absolute values of the transfer function, b_5 and b_9 are all different from the canonical design values by varying amounts, due to the "soft" coils of this magnet.

Figures 7 thru 9 show the lowest three non-allowed harmonics as measured for this magnet. The sizable skew sextupole and decapole components are generated by distortions in the "soft" coil package, and will be brought under control in forthcoming magnets.

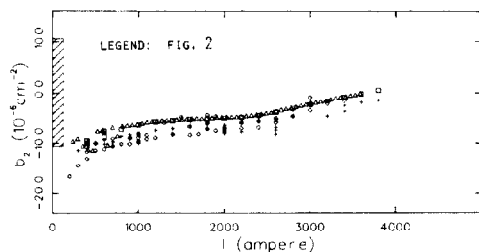


Fig. 7a. Normal sextupole coefficient.

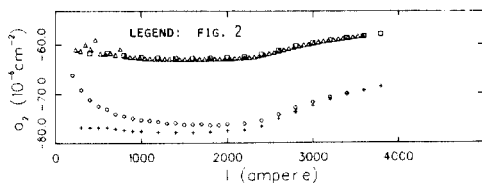


Fig. 7b. Skew sextupole coefficient.

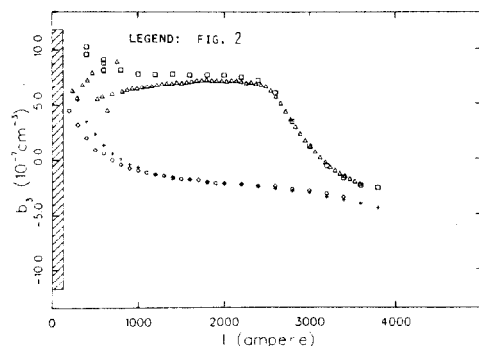


Fig. 8a. Normal octupole coefficient.

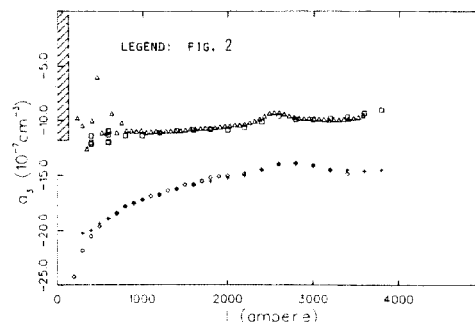


Fig. 8b. Skew octupole coefficient.

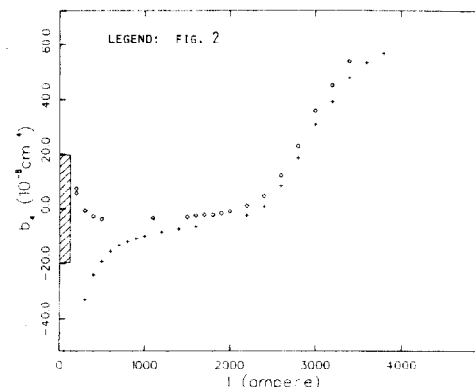


Fig. 9a. Normal decapole coefficient.

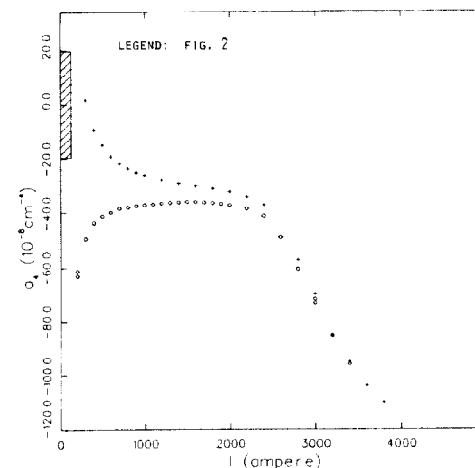


Fig. 9b. Skew decapole coefficient.

References

1. Design given in: P.F. Dahl & H. Mahn, "Proposed Pre-Production Quadrupole Design", Internal Report TN 154, unpublished.
2. The construction and performance characteristics of the earlier quadrupoles MQ3001 and MQ4001 have been detailed in: R. Engelmann, A.F. Greene, J. Herrera, K. Robins, and E. Willen, "Construction & Field Characteristics of Early ISABELLE Quadrupoles MQ3001 & MQ4001", Internal Report TN 260, unpublished.
3. G.H. Morgan, Proc. 4th Inter. Conf. on Magnet Tech., Brookhaven, 787 (1972).
4. The design parameters for ISABELLE are listed in the ISABELLE PARAMETER LIST, 5/2/80, unpublished.
5. T. Luhman, "Metallurgical Characterization of NbTi Braid for ISABELLE", Internal report TN 274, unpublished.